P3.4 DIAGNOSIS OF PHASE ERRORS IN HIGH-RESOLUTION NWP MODEL FORECASTS OF PRECIPITATION AND APPLICATION TO IMPROVED AVIATION WEATHER FORECASTS

C. Phillips, J. Pinto, M. Steiner and D. Albo
NCAR/Research Applications Laboratory
Boulder, Colorado, USA

1. INTRODUCTION

Accurate and highly resolved forecasts of aviation weather hazards are needed by today's air traffic flow planners and the automated decision support tools of NEXTGEN. Both current users and NEXTGEN require information about the likely distribution of storm sizes, their intensities, organization, connectedness, and orientation to make better-informed air traffic routing decisions up to eight hours in advance (depending on the length of the route).

Toward meeting these requirements, an advanced storm prediction algorithm called CoSPA has been developed. CoSPA is a collaboration between the National Center for Atmospheric Research (NCAR), the Massachusetts Institute of Technology Lincoln Laboratories (MIT-LL), and the National Oceanic and Atmospheric Administration (NOAA). CoSPA is funded by the Federal Aviation Administration (FAA). The goal of CoSPA is to produce a rapidly updating short-term forecasting system that optimally blends heuristic extrapolation forecasts with high-resolution model forecast data. Details of CoSPA and recent enhancements are given in Dupree et al. (2009) and Pinto et al. (2010).

An important aspect of the blending is the alignment of the nowcast with the model forecast prior to the blending. This is done by comparing model forecast images to the most recent available observations and determining the offset or phase shift between the two images. The work presented in this paper describes the methodology for producing the phase correction vectors and the optimization of parameters used in the calculations.

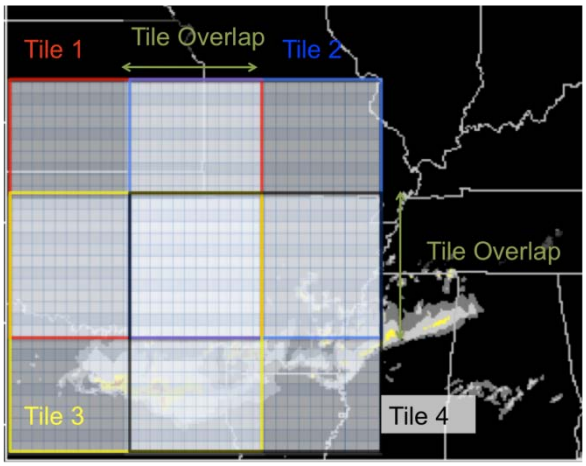

Figure 1. Example of tiles and tile overlap. Each individual tile is outlined with a different color. The smaller grid within each box is the low_res grid.

2. METHODOLOGY

The data used in this study are MIT-LL CIWS VIL analysis mosaic and forecasts from the rapidly-updating High-resolution Rapid Refresh (HRRR) model run at NOAA/GSD.

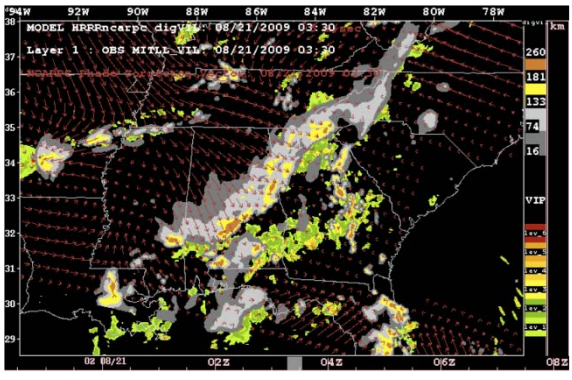

Figure 2. Phase correction vectors used to match the model (top layer) with observations (bottom layer).

CIWS data are available every 2.5 min at 1 km resolution. These data are sub-sampled in space

and time to 15 min and 3 km, respectively. The data are re-gridded to the model grid using a Cressman distance weighted average interpolation approach.

The HRRR model is currently being run experimentally by NOAA/GSD. The HRRR uses the ARW core of the Weather Research and Forecasting (WRF) model at 3-km resolution without convective parameterization. It is initialized and driven at the lateral boundaries with the 13-km Rapid Update Cycle (RUC). Forecasts are generated every hour with output at 15-min lead times out to 12 hours. The model VIL data are calibrated using a frequency matching technique (see Pinto et al. 2010) and converted to the same digital scale (0-255) as the CIWS observed VIL mosaic. This calibration procedure is done so that the distribution of intensities in the model and the observations are similar.

Position errors in the model forecasts are then determined using a method described previously by Brewster (2004) which is further detailed below.

2.1 PHASE CORRECTION DESCRIPTION

A technique originated by Brewster (2004) is used to correct position errors in the HRRR model forecast. For each model generation time, the phase correction is performed at a lead time of 3 hrs (due to HRRR latency of 3 hrs). Then that calculated correction is applied to the rest of the lead times from that generation time out to 8 hrs.

Before phase correcting, the model and observations are smoothed and sub-sampled to reduce computation time. Sub-sampling is controlled by a parameter called “low_res”, which is the resolution of the sub-sampled grid (Table 1).

The model domain is then divided into N tiles, where N is determined by the tile size, the overlap, and the size of the domain. The tile overlap is typically about half of the tile size (see Figure 1). Each tile is shifted in both x and y directions using an increment of dx = dy and a maximum shift distance of M_s. After each tile is shifted, the squared difference between the shifted model field, F(x+dx) and the observations, O(x) is computed and weighted by a distance penalty, D (see Brewster 2004 for description).

$$J(dx) = D \sum_{i=1}^{n} \{F(x_i + dx) - o_i(x_i)\}^2$$

Scores are calculated for each possible shift of a particular tile. The shift with the minimum score gives the phase correction vector for that tile. This minimization is performed for each tile across the entire model grid. A final smoothing step is performed on the resulting grid of phase vectors resulting in a smoothly-varying gridded product (see Figure 2).

Variable	‘09 Value (km)	Optimized (km)
obs_input_smooth	27	27
forecast_input_smooth	27	27
low_res	15	9
tile_size	300	200
tile_overlap	150	100
max_phase_shift	240	100
phase_shift_res	60	55
max_phase_shift_refinement	45	220
phase_shift_res_refinement	15	9
Max_phase_shift_res_refinement	45	45
good_dist_scaling	1.5	1.5
good_scaling	2	2.0
Threshold (dVIL)	20	20
variance	NA	NA
high_res_output_fcst_smooth	9	9
low_res_motion_smooth	9	9

Table 1. All optimized phase correction parameters

2.2 PHASE CORRECTION OPTIMIZATION

For phase correction optimization, various parameters were adjusted in numerous case studies over the summer of 2009. Table 1 lists the values used for the summer of 2009 and the optimized values after extensive testing. Some of the more important variables in this study are low_res, tile_size, tile_overlap, phase_shift_res, and threshold. Examples of the process by

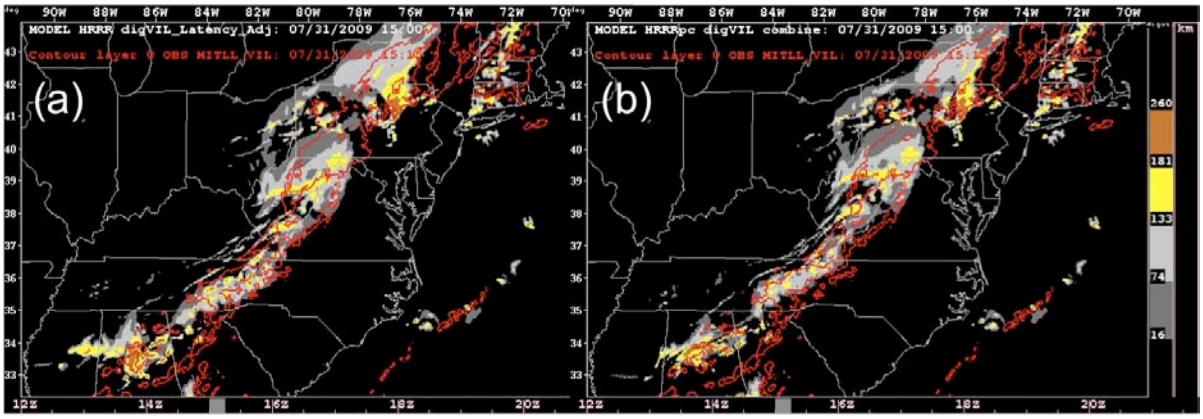

Figure 3. 31 July 2009. 2-hr HRRR forecast (forecast image) and observations (outlined in red) (a) without phase correction and (b) with phase correction.

which the phase correction was optimized are given in the Case Studies section.

3. CASE STUDIES

31 July 2009 – Line Storm

A prominent line storm was situated over the eastern part of the continental US (CONUS) on this day, causing delays in excess of 3 hrs at some airports. Figure 3a shows a 2-hr forecast from the HRRR model with no phase correction overlaid on the observations. In Figure 3b, phase correction has been applied, correcting some of the errors in the forecast while still depicting a physically and visually realistic forecast. Note the correction of false alarms over the southwestern part of the map.

Critical Success Index (CSI) and bias scores for all model generation times sorted by lead time are plotted in Figure 4. Low_res9 and Low_res15 represent a sub-sampled grid spacing of 9 and 15 km, respectively; "combine" identifies the phase correction calculated using all optimized parameters shown in Table 1; and No Phase Correct is solely the HRRR model with no phase correction. The CSI scores exhibit that more skilful forecasts are a function of decreasing the sub-sampled grid spacing. It is also important to note that the combined set of optimized variables is the most skillful. Thus, optimizing all variables together provides a cumulatively improved forecast.

A decrease in the bias by each of the phase correction tests can be seen in the first 4 hrs of the forecast lead times. The phase correction sometimes tends to over-correct the model, converging many vectors into one spot and causing areas of convection to seemingly "disappear." A convergence algorithm is currently being developed to mitigate this problem.

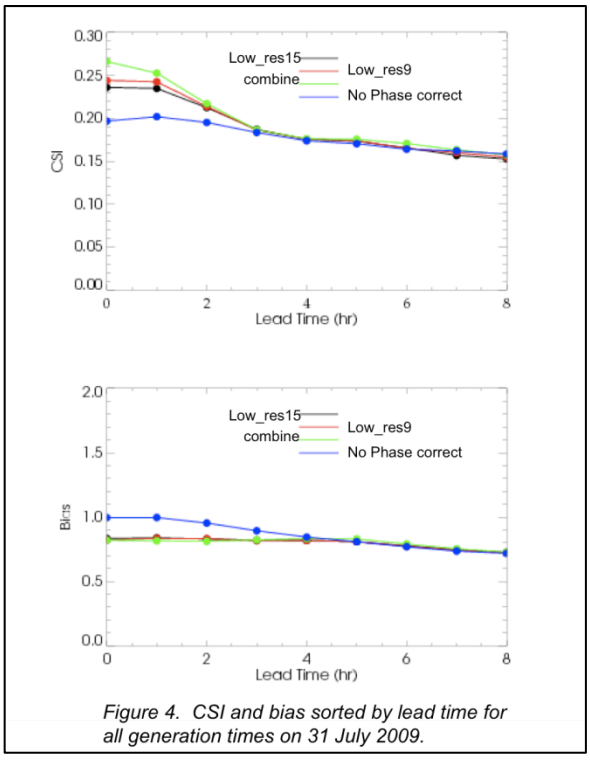

Figure 4. CSI and bias sorted by lead time for all generation times on 31 July 2009.

11 June 2009 – Low Pressure

A strong low pressure system was centered over the Illinois/Indiana border on this day. Airport delays were reported across the country because of this storm. Figure 5a shows the 2-hr HRRR forecast initialized at 10 UTC overlaid by the 12 UTC observations. Note the HRRR's over-expanding of convection in this area. Figure 5b shows the model forecast after phase correction has been performed. The phase correction diagnoses the errors in the forecast

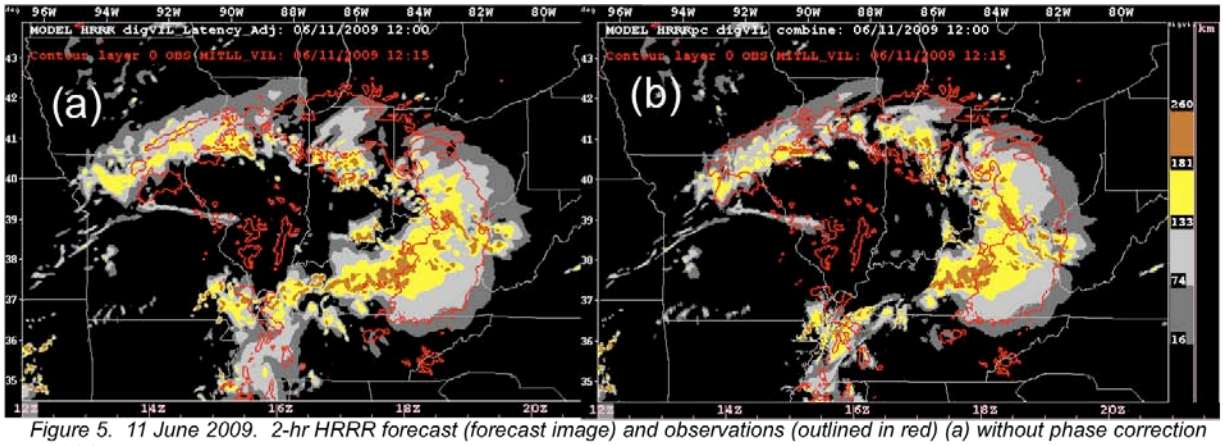

Figure 5. 11 June 2009. 2-hr HRRR forecast (forecast image) and observations (outlined in red) (a) without phase correction and (b) with phase correction.

and corrects accordingly, reducing the area of the convection to match the observations.

Figure 6 shows the CSI and bias scores of various threshold sensitivity tests. Lowering the threshold proves to be more skilful here while combining the optimized parameters again provides the best forecast in earlier lead times. No phase correction outputs the least skilful forecast once again.

4. SUMMARY / FUTURE WORK

Brewster's phase correction technique can be a useful tool for correcting position errors in forecasts, especially in earlier lead times. It seems to be most valuable for large, organized systems with continuous convection over large areas. The algorithm tends to improve skill scores by reducing the bias. This bias reduction occurs to excess at times (as seen in Figure 4). Current work is underway to mitigate this problem by reducing the amount of convergent motion allowed in the phase error field.

In the tests done for this study, an Eurlerian approach was taken, wherein corrections were developed by comparing the model with the observations at a single forecast lead time and applying to all forecast lead times. Future versions of the phase correction will employ a Lagrangian technique, in which the corrections will take into account motion of the precipitation areas as well as trends in the phase errors.

Acknowledgements. This research is in response to requirements and funding by the Federal Aviation Administration (FAA). The views expressed are those of the authors and do not necessarily represent the official policy or position of the FAA.

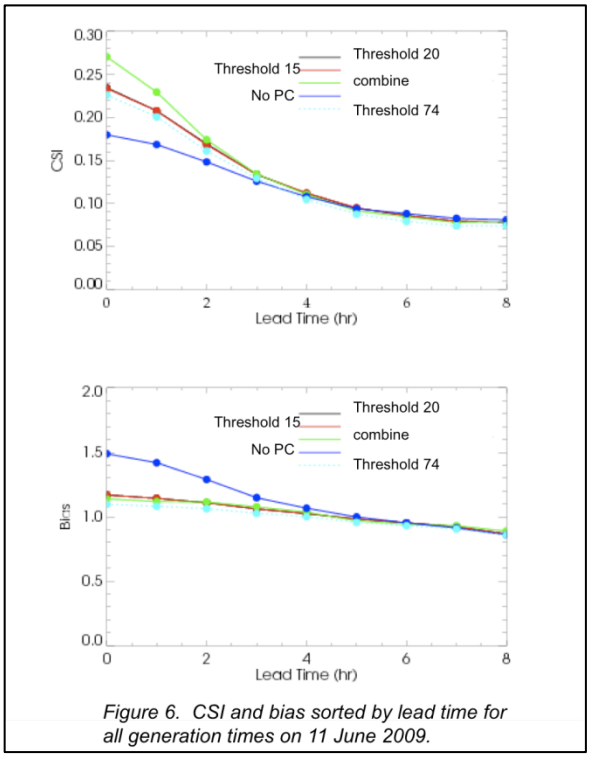

Figure 6. CSI and bias sorted by lead time for all generation times on 11 June 2009.

5. REFERENCES

Brewster, K.A., 2004: Phase-correcting data assimilation and application to storm-scale numerical weather prediction. Part I: Method description and simulation testing. *Mon. Wea. Rev.*, **131**, 480-492.

Dupree, W., et al., 2009: Advanced Storm Prediction for Aviation Forecast Demonstration. *WMO Symposium on Nowcasting*, Whistler, BC, Canada, 19 pp.

Pinto J., W. Dupree, S. Weygandt, M. Wolfson, S. Benjamin, and M. Steiner, 2010: *AMS 14th Conference on Aviation, Range, and Aerospace Meteorology (ARAM)*, Atlanta, GA